45th AIAA/ASME/SAE/ASEE Joint Propulsion Conference & Exhibit
2 - 5 August 2009, Denver, Colorado

AIAA 2009-5448

Effects of Inductive Coil Geometry in the Conical Theta Pinch Faraday Accelerator with Radio Frequency Assisted Discharge

Ashley K. Hallock* and Edgar Y. Choueiri†

Princeton University, Princeton, NJ, 08544

The effects of inductive coil geometry on current sheet velocity in a conical theta pinch acceleration stage were explored through experiments and calculations in order to obtain insight into optimizing the coil geometry for the theta pinch Faraday accelerator with radio frequency assisted discharge (CΘP-FARAD). The experiment consisted of carrying out static measurements of the mutual inductance between a set of conical inductive coils of varying lengths and half-cone angles and their associated currents sheet analogs made out of metallic foil. The measured dependences of mutual inductance on the axial distance between the coil and the sheet were used as input to an analytical circuit model of inductive current sheet acceleration. This allowed the inference of some of the effects of coil geometry on the performance of the accelerator (the final sheet velocity). It was found that shorter driving coils, and to a lesser extent larger half-cone angles (whose effects are less pronounced for longer coils), are more favorable for vigorous current sheet acceleration. The trends were explained by considering that the uniformity of the magnetic field within the volume of a coil increases for longer, more solenoidal coils, and therefore would present a reduced magnetic field gradient to a current sheet translating away from the coil, thus reducing the rate of the change of inductance with distance and consequently decreasing the final sheet velocity.

Nomenclature

C	capacitor capacitance, μF	v_z	axial velocity, km/s
I_1, I_2	driving coil current, plasma current, Amps	z_0	decoupling distance, m
L_0, L_C	initial, coil inductance, nH	z	axial displacement, m
l	coil length, cm	α	cone half angle, degrees
M	mutual inductance, nH	η	efficiency
m	mass, kg	ϕ	flux, weber
R_p	plasma resistance, ohms	ρ_A	linear mass density, kg/m

I. Introduction

Pulsed inductive thrusters[1] are a specific class of electrodeless thrusters under development for use in space propulsion applications. Electrodeless thrusters are attractive because of their avoidance of the lifetime-limiting issues associated with electrode erosion. In addition, they can process propellants such as CO_2 and H_2O that are incompatible with metallic electrodes.

These thrusters operate by discharging a short, high-current pulse through an inductive coil, producing a time-changing magnetic field that induces an electric field in accordance with Faraday's law. The propellant

*Graduate Student, Mechanical and Aerospace Engineering Department, E-Quad Olden St. Princeton, NJ 08544, Student Member AIAA.

†Chief Scientist of the Electric Propulsion and Plasma Dynamics Lab (EPPDyL) and Professor, Mechanical and Aerospace Engineering Department, E-Quad Olden St. Princeton, NJ 08544, Fellow AIAA

breaks down (ionizes) near the inductive coil, where the induced fields are sufficiently strong, and a current sheet forms with current flowing in the opposite direction to that of the current in the inductive coil. When the opposing current loops are close to each other they can be seen as a transformer, coupling the plasma to the driving circuit. The high magnetic pressure that exists between the plasma current sheet and the inductive coil can potentially accelerate the current sheet and any entrained propellant away from the coil to produce thrust, as long as the relevant scaling parameters are kept within the optimum range of values.[2] If the thruster design does not ensure the proper values for these parameters, the current sheet may remain coupled to the driving circuit, or never form at all. Optimizing current sheet formation can therefore greatly improve the performance of this type of thruster.

The current rise rate in the plasma is a critical parameter because the faster the current rises in the current sheet, the smaller is the separation between driving coil and current sheet when the current sheet is fully-formed and the better is the inductive coupling between the two.

One way to hasten current sheet formation is through the use of a preionized propellant,[3] which will also significantly reduce the required capacitor voltage and pulsed energy for forming and accelerating the sheet. Choueiri and Polzin[4] introduced the Faraday Accelerator with Radio-frequency Assisted Discharge (FARAD) to demonstrate the concept of preionization-assisted low discharge energy inductive current sheet formation. They have performed proof-of-concept experiments, developed design criteria,[2] and identified potential advantages a FARAD thruster might enjoy over the current state-of-the-art Pulsed Inductive Thruster (PIT),[1,5,6] which relies on injecting a neutral gas onto the coil from a valve positioned downstream inside the plasma jet. Although the use of preionization adds complexity to the system, it can also help to eliminate complexity elsewhere, yielding a system that is, on balance, simpler and more compact. The proof-of-concept experiments were successful in demonstrating preionization-assisted current sheet formation at significantly lower capacitor voltages and pulse energies than those found in the PIT (1.5 kV and 44J versus 30kV and 4kJ).

In previous FARAD experiments, propellant reached the flat inductive coil surface from a preionization chamber located upstream of the coil. This required the use of a strongly cusped magnetic field to impose an almost ninety degree turn on the preionized propellant stream. Turning the propellant at such high angles was a difficult process, which motivated the design of an inductive coil that more naturally follows the diffusive path of the preionized gas, resulting in the Conical Theta Pinch FARAD (CΘP-FARAD),[7] shown in Fig. 1. The CΘP coil geometry is the sole difference between CΘP-FARAD and the original FARAD used in previous proof-of-concept experiments.

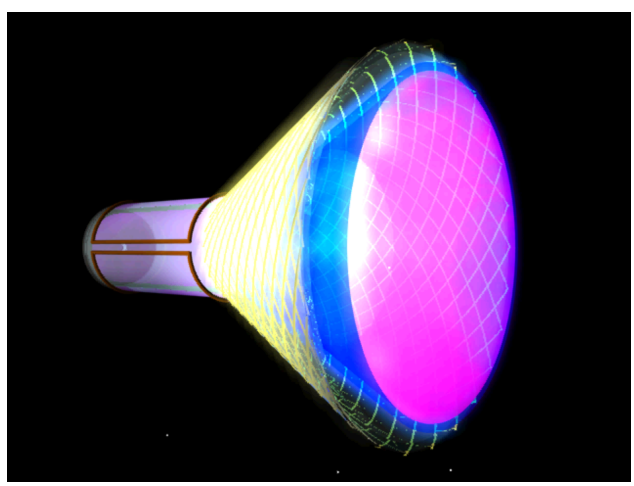

Figure 1. Conical Theta Pinch FARAD with preionization chamber to the left and current sheet shown in blue.

Coil geometry affects current sheet formation through the mutual inductance (M) between the driving coil and the current sheet. Mutual inductance between two coils is defined as the amount of magnetic flux flowing through the second coil divided by the current flowing through the first, multiplied by the number of turns in the first:

$$M_{21} = \frac{n\phi_{21}}{I_1}, \tag{1}$$

and since ϕ_{21} scales linearly with I_1, the mutual inductance is purely a function of the geometry and not the current.

The further the current sheet forms from the inductive coil, the lower the initial mutual inductance will be, causing a larger initial inductance to be presented to the driving circuit due to the current sheet's inability to shield out the field from the driving coil. The initial inductance presented to the circuit affects the efficiency of pulsed inductive-type thrusters according to the Lovberg criterion, which states that the efficiency is limited by the ratio of the total change in inductance to the initial inductance:[8]

$$\eta \leq \frac{\Delta L}{L_0} \tag{2}$$

Therefore, to achieve the most efficient operation, initial shielding of the inductive coil's magnetic field by the current sheet must be maximized in order to allow for the maximum possible change in inductance as the current sheet moves away from the driving coil. This translates into an initially high mutual inductance between the driving coil and the plasma current sheet, however, if the mutual inductance remains high as the current sheet progresses away from the driving coil, the current sheet may remain coupled to the driving circuit at the time when the the driving current reverses direction and begins removing energy from the current sheet. A balance must be reached with respect to the decrease in mutual inductance as a function of current sheet and driving coil separation such that the current sheet remains coupled until fully-formed, and then rapidly decouples before the driving current reverses direction.

In order to investigate this dependence, and more explicitly, the effects of coil geometry on mutual inductance, we constructed six inductive coils of differing half-cone angle and length and experimentally determined the mutual inductance between each coil and a current sheet replica as a function of the axial separation of the two. The "current sheets" were made of aluminum and with the same geometry as the driving coil.

We then obtained curve fits to the experimentally-determined mutual inductance versus position dependence, $M(z)$, for each of the six coil geometries, and used those fits as an input to the well-known model of the PIT[8,9] in lieu of the previously used expression for $M(z)$ that was obtained empirically for the case of a 90 ° half-cone angle (i.e. the flat coil of the PIT). This allowed us to use calculations obtained from the model to draw conclusions about how the inductive coil geometry affects the performance, which in the context of this paper is defined as the final current sheet velocity.

Figure 2. ***Left:*** **Photograph showing a current sheet analog on the left and a driving coil with 10° half-cone angle, a length of 5 cm, and a minor radius of 3 cm to the right. and** ***Right:*** **An example of a computer-generated image from a gerber file.**

The remainder of this paper is organized into successive sections in which we describe the experiment, report mutual inductance measurements, discuss the observed trends and, with the use of a model, extract physical insight into some of the basic influences of coil geometry on thruster performance.

II. Experimental Setup

A. Driving Circuit and Current Sheet Construction

We constructed models of the inductive coil with half-cone angles of 10°, 20° and 30°, and produced inductive coils of two different lengths for each angle (5 and 10 cm). All coils had a minor radius of 3 cm. A photograph of the coil of 10° half-cone angle and 5 cm length and its associated current sheet analog (made out of aluminum foil as described in the next subsection) is shown in the left side of Fig. 2. Since mutual inductance is purely a function of geometry, and does not depend on the amount of current, the models were constructed at full-size but for low-energy operation only, allowing fast and inexpensive construction.

Gerber files, used for printing circuit boards, were written to produce the exact patterns that will be used in the full-scale construction of higher-energy driving coils. The right side of Fig. 2 shows an example of the image produced by a program that reads the Gerber files. These patterns, which are calculated to create a purely azimuthal current density along the surface of the inductive coil,[8] are printed on two sides of printer paper and the traces filled in with conductive ink. The wide trace that extends nearly the entire length of the coil is where current is fed to the circuit, and the circles at the edge of the circuit are the locations where current transfers from one side of the circuit to the other.

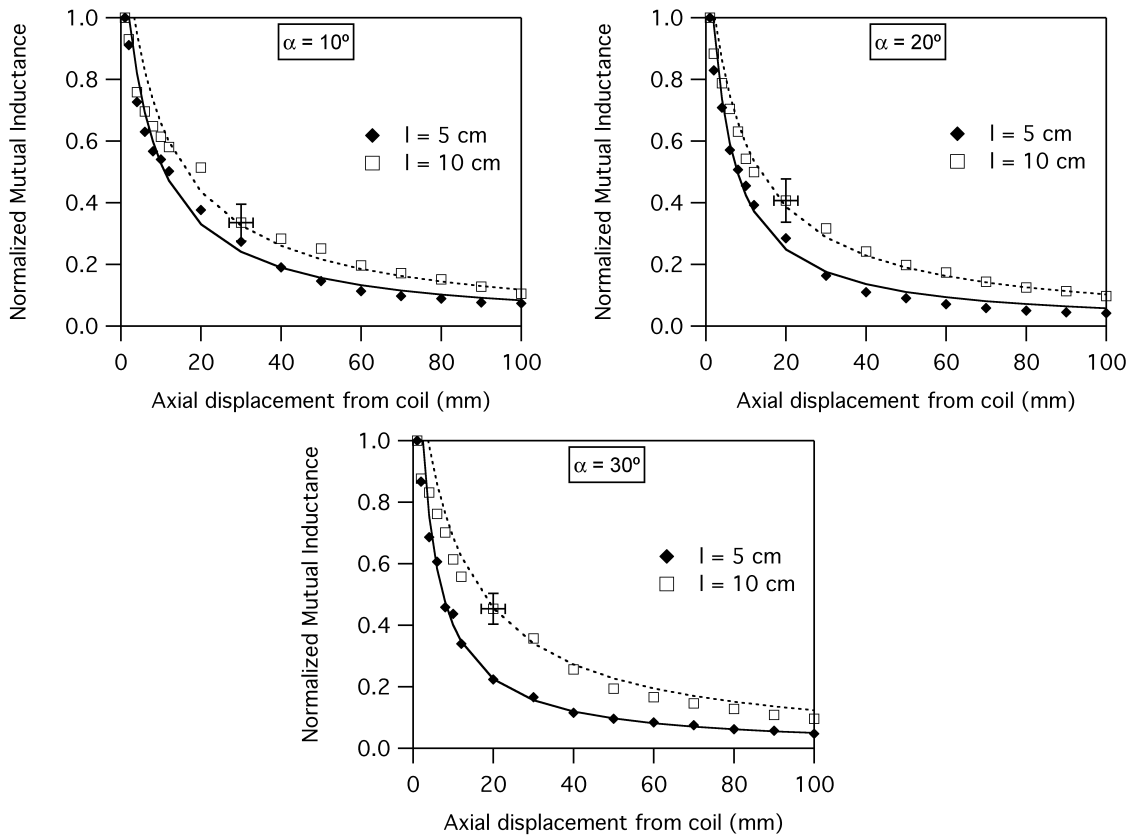

Figure 3. Mutual inductance between the inductive coils of 5 and 10 cm long and (from left to right, top to bottom) 10, 20 and 30 degree half-cone angle and their associated current sheets as a function of axial separation distance, normalized to the value at the smallest separation distance. Markers indicate experimental data, lines represent a fit to the data.

B. Position-dependent Mutual Inductance Measurements

A function generator provided current to the driving circuit in the form of a sine wave, whose frequency was set to the expected frequency of the full-scale circuit (50 kHz). The inductance shown to the driving circuit changes as a function of time due to the motion of the current sheet away from the driving coil. In order to simulate this effect, aluminum foil was wrapped around a supporting structure identical to that supporting

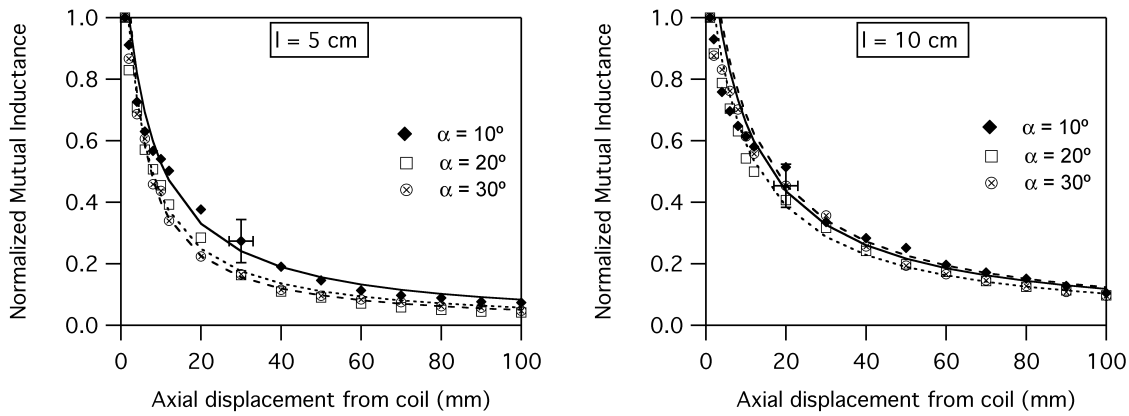

Figure 4. Mutual inductance between the inductive coils of 10, 20 and 30 degree half-cone angle and (left to right) 5 and 10 cm cone length and their associated current sheets as a function of axial separation distance, normalized to the value at the smallest separation distance. Markers indicate experimental data.

the driving coil. The aluminum foil does not completely circumnavigate the supporting cone, leaving a space across which induced voltage may be measured. This induced voltage is a measure of the mutual inductance of the primary coil to the current sheet replica, and decreases as the current sheet replica moves further away from the driving coil. It is this decoupling that affects the inductance presented to the driving circuit. In the most efficient case, the current sheet will completely shield the field of the driving coil (a coupling coefficient of 1). When the current sheet moves away from the driving coil, the mutual inductance should reduce in such a way that the current sheet decouples from the driving coil before the time derivative of the current reverses sign in the driving circuit (at a quarter period) but after significant energy has been transferred from the driving coil to the current sheet.

III. Experimental Results

In this section we present plots, shown in Fig. 4, of the measured mutual inductance between the driving coils and current sheet replicas for different geometries. The mutual inductances are normalized to their value at the smallest separation distance between the driving coil and the current sheet replica.

A function of the form

$$M^* = \frac{l}{Az + Bl} \tag{3}$$

was found to provide a good fit to the data where different values of A and B correspond to different geometries, M^* is the non-dimensional mutual inductance (normalized to the initial value), l is the length, and z is the axial displacement of the current sheet away from the driving coil. This fit, which has an R^2 value of greater than 99.90% for all data, is shown as lines in Fig. 4. Values for A and B for the different geometries are given in Table 1.

Table 1. Fit Coefficients to the Experimental Data for the Various Geometries Studied

l (cm)	α (degrees)	A	B
5 cm	10°	6.7	0.52
5 cm	20°	8.3	0.69
5 cm	30°	9.8	0.54
10 cm	10°	7.7	0.75
10 cm	20°	8.9	0.80
10 cm	30°	7.4	0.72

It can be seen from these plots that for all three half-cone angles, the mutual inductance decreases more rapidly for shorter cone lengths. In addition, the difference between the curves for the two lengths increases,

on average, as the half-cone angle increases. For 10°, the average difference in normalized mutual inductance is 0.07 ± 0.007, for 20° it is 0.09 ± 0.009 and for 30° it is 0.16 ± 0.015. When the data for $M(z)$ are plotted for all half-cone angles for a given length on the same plot, we see that there is no noticeable difference, within the error bars, between the $M(z)$ dependences for the three half-cone angles with longer coils (right panel of Fig. 4, but such a difference is noticeable for the shorter coils (left panel of the same figure) where $M(z)$ appears to drop off more rapidly with z for higher cone angles. However, results of a Student t-test performed on the coefficients of the fit indicate that any variation between them cannot be statistically discriminated from the noise associated with the measurements with a certainty greater than 90%. Therefore, we restrict our conclusions on the effect of half-cone angle on $M(z)$ to the relative difference in $M(z)$ for the two cone lengths as mentioned above.

In order to understand the effects of inductive coil geometry on the final current sheet velocity, the data fits for the experimentally-measured $M(z)$ relations are used as the mutual inductance input to the analytical model of inductive current sheet acceleration described in the next section.

IV. Model

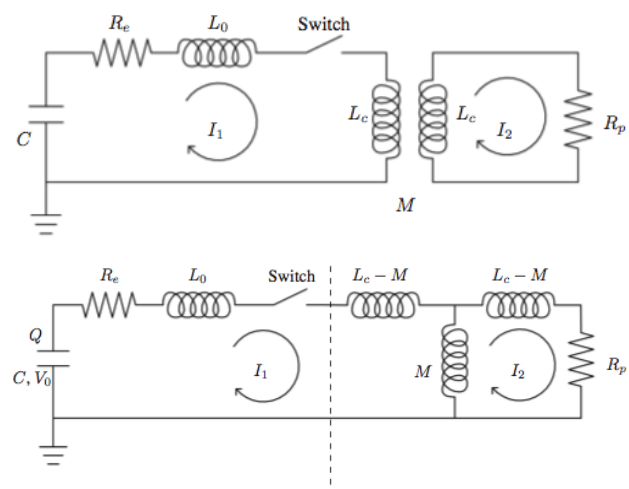

Figure 5. Lumped circuit diagrams representing the driving circuit coupled to the plasma.

The model discussed in this section has been described[2,8,9] in detail and used to model the two predecessors to this thruster. It is a circuit analog model of pulsed inductive acceleration. In this paper we use the model to link the experimental data of mutual inductance as a function of driving coil-current sheet separation distance to thruster performance, defined here as final current sheet velocity, in order to be able to arrive at conclusions about the effects of geometry on current sheet acceleration.

The driving circuit, inductive coil, and current sheet can be modeled as two coupled lumped-element circuits (shown in Fig. 5), with the inductive coil and current sheet acting as a transformer.

A. Governing Equations

The following equations can be written from these circuits:

$$\frac{dI_1}{dt} = \frac{\frac{L_C}{V} - L_C R_e I_1 - M R_p I_2 + (L_C I_2 + M I_1)\frac{dM}{dt}}{L_C\left(L_0 + L_C\right) - M^2} \tag{4}$$

$$\frac{dI_2}{dt} = \frac{M\frac{dI_1}{dt} + I_1\frac{dM}{dt} - R_p I_2}{L_C} \tag{5}$$

$$\frac{dV}{dt} = -I_1/C \tag{6}$$

where I_1 is the current flowing in the driving circuit, I_2 is the current flowing in the plasma current sheet, C is the capacitance of the capacitor, M is the mutual inductance between the driving coil and the current

sheet, L_0 is the initial inductance in the driving circuit, L_C is the coil inductance, R_p is the resistance of the plasma, and V is the voltage on the capacitor.

With the use of the circuit diagrams, the coil inductance can be written as:

$$L_{term} = L_C - \frac{M^2}{L_C}. \tag{7}$$

It can be seen from this equation that the coil inductance changes as a function of time due to the time changing mutual inductance, which changes due to the time changing nature of the position of the current sheet. An expression for the mutual inductance as a function of current sheet axial position has been empirically determined for a half-cone angle of 90°[8,9] (i.e. flat coil):

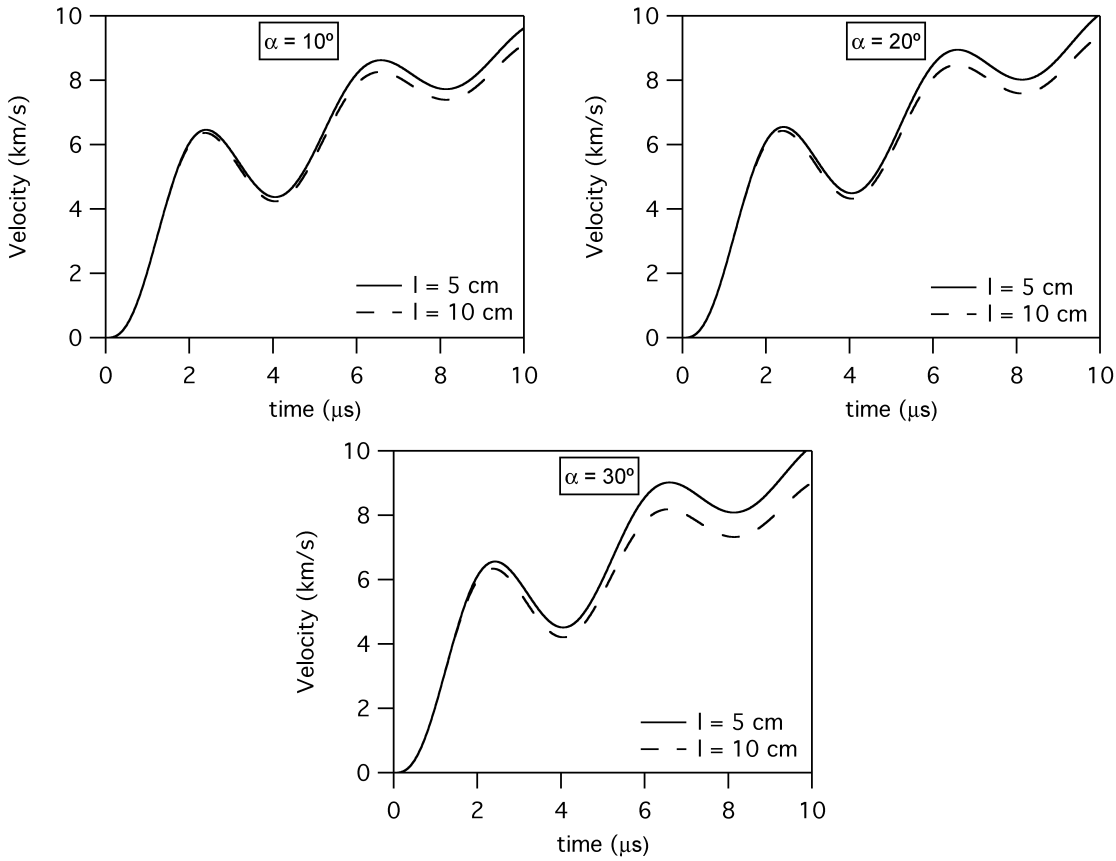

Figure 6. Results from the model for the six different geometries studied.

$$L_{tot}(z) = L_0 + L_C\left(1 - \exp\left(-z/z_0\right)\right) = L_0 + L_{term} \tag{8}$$

where z is the axial displacement of the current sheet from the driving coil, and z_0 is the decoupling distance. This expression is set equal to the previous expression for total inductance, and solved to produce an equation for the mutual inductance that is a function of driving coil and current sheet separation distance and of which the time derivative can easily be taken:

$$M = L_C \exp\left(-z/2z_0\right) \tag{9}$$

This empirical relation, derived for a half-cone angle of 90°, is replaced by Eq. 3 in order to use the model presented here to predict how the geometries from the experiment described above will affect current sheet dynamics.

The equation of motion for the current sheet can be written taking into account the force acting on the current sheet due to the magnetic pressure between the driving coil and the current sheet as well as the

accumulation of propellant mass according to a snowplough model.

$$\frac{dv_z}{dt} = \frac{1}{m(z)}\left[\frac{L_C I_1^2}{2z_0}\exp\left(-\frac{z}{z_0}\right) - \rho_A(z)\, v_z^2\right] \tag{10}$$

where ρ_A is the linear mass density distribution and v_z is the axial current sheet velocity. A simple velocity definition closes this set:

$$\frac{dz}{dt} = v_z \tag{11}$$

For this study, the accelerating force was modeled as a simple axial Lorentz force and the pressure was modeled as a constant backfill at a value that is within the range of efficient operation as described in a previous study of the effect of pressure and pulse energy on current sheet formation.[10] The coil inductance was varied over an order of magnitude (from $\mathcal{O}$ ∼100 nH to $\mathcal{O}$ ∼1000 nH) with no noticeable change in the resulting trend in mutual inductance, current sheet velocity or position.

B. Solutions

In this section we present in Fig. 6 solutions of the model described in the previous section. These results correspond to the six different geometries studied, where Eq. 9 was replaced by Eq. 3 with the corresponding coefficients for the particular geometry. The decreases in velocity correspond to changes in the slope of the driving coil current.

These plots show that, for the parameter space studied, the thruster can accelerate the current sheet to a higher velocity for geometries that cause the mutual inductance to drop most rapidly as a function of the current sheet's axial displacement from the driving coil. The results also show that the difference in final velocity for the two different lengths is greater for larger cone angles than for smaller ones. This is consistent with the trends in $M(z)$ seen in the experimental data.

V. Discussion

Combining the results of the experiments and the results of the model we conclude that shorter inductive coils will cause the mutual inductance to decrease faster as a function of driving coil and current sheet separation, and will in turn accelerate the current sheet to a higher velocity within the same period of time.

An explanation for the more gradual decrease in mutual inductance as the current sheet moves axially away from the driving coil can be seen by referring to the simulated magnetic field patterns associated with the two different coil lengths (shown in Fig. 7) for a driving current amplitude of 20,000 Amps. These simulations were obtained using the program Maxwell SV by Ansoft to simulate a current flowing through a conical conductor made of copper having the same geometry as the inductive coils studied here.

If we assume that magnetic flux is conserved through the interior of the driving coil, then the field for longer coils will be more solenoidal, or constant, within the volume of the coil, and transitions to a $B \sim 1/z^3$ dependency will occur at larger values of z. This is consistent with a more-quickly decreasing flux within the current sheet due to the driving coil as the current sheet progresses axially away from the driving coil.

The effect of half-cone angle on the results of the model are limited to causing a greater disparity in velocity for different cone lengths as the half-cone angle is increased. The fact that the length has a greater effect on $M(z)$ can be explained by comparing how the magnetic field profile within the volume of the cone changes with cone angle and how the profile changes with length. In Fig. 7, the magnetic field changes more dramatically between shorter and longer coils than for coils of differing half-cone angle. It should be noted that the field profile does change with cone angle, but over the parameter space studied here, the effect is too small to be observed in our experiment.

VI. Conclusions

Experimentally determined relations for the mutual inductance between driving coils of varying geometries and associated current sheet analogs reveal that the length of the driving coil affects the dependence between mutual inductance and axial separation distance between the two coils. Longer coils will cause the mutual inductance to drop off less rapidly with separation distance, which can be understood considering the magnetic field patterns associated with these two geometries. For longer coils, the more-uniform section of

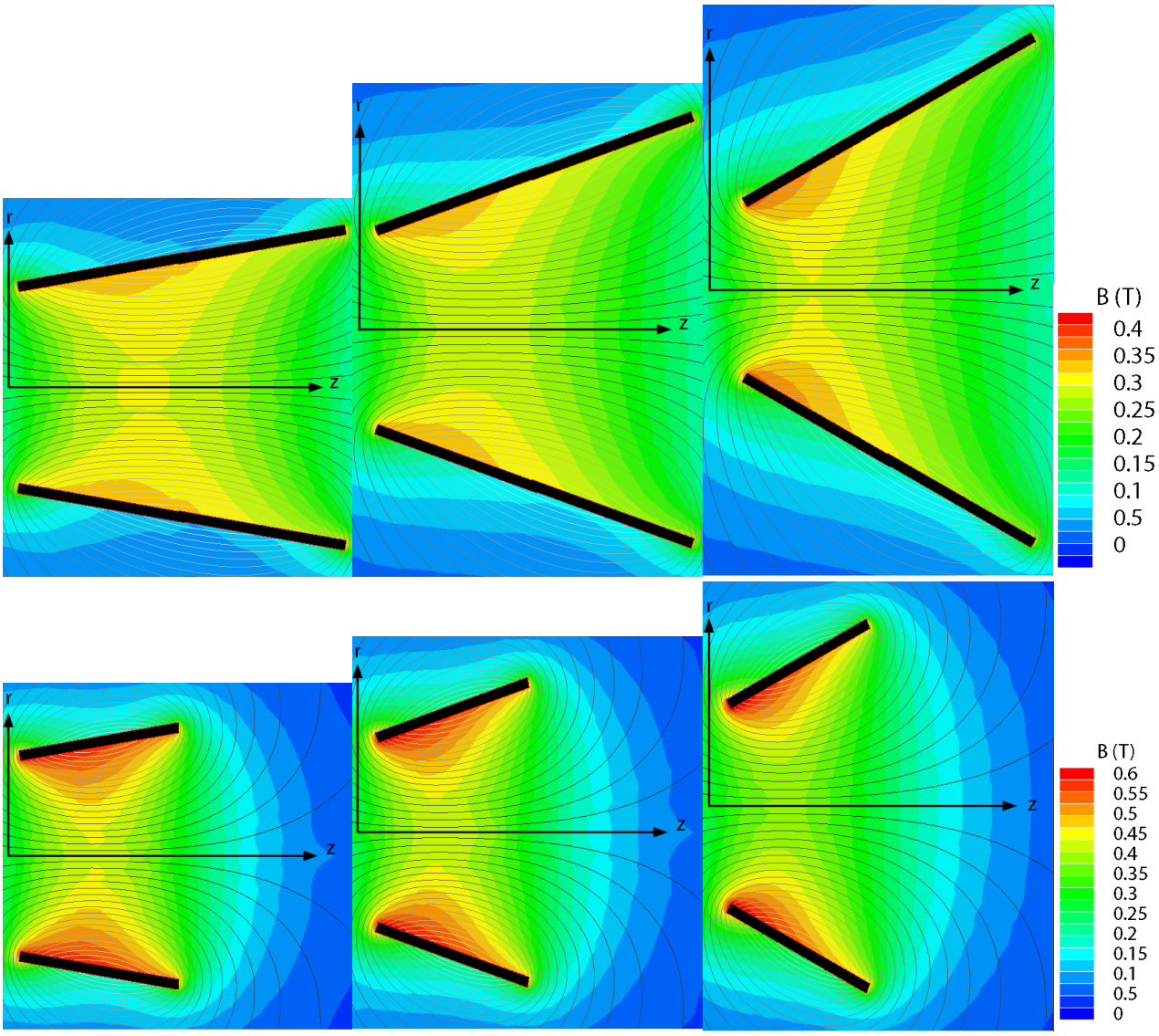

Figure 7. Simulations of the magnetic field (performed in Ansoft Maxwell SV) (left to right) 10°, 20°, and 30° half-cone angle, for *Top Row:* a length of 10 cm and *Bottom Row:* a length of 5 cm.

the field will be extended through the interior of the coil, and the gradient in magnetic field strength within the volume of a current sheet translating axially away from the driving coil will be reduced over that of a shorter driving coil. As the half-cone angle is increased, the disparity in the magnetic field profile within the volume of the current sheet for differing lengths is greater, causing the difference in $M(z)$ for the two cone lengths to be larger for larger half-cone angles, but conclusions on the influence of half-cone angle on $M(z)$ are limited to this relative effect as half-cone angle has a less dramatic impact on the magnetic field profile than coil length.

We conclude that, within the parameter space investigated and the assumptions of the model, shorter driving coils, and to a lesser extent larger half-cone angles (whose effects are less pronounced for longer coils), are more favorable for higher current sheet acceleration.

Both the experiment and the model do not take into account the radial compression of the current sheet that occurs due to the pinching effect of a real thruster. The extent to which that pinching may alter the above conclusions should be the subject of a future investigation.

Acknowledgments

This research project is carried out under a contract from the the Air Force Office of Scientific Research. We also acknowledge support from the Plasma Science and Technology Program from the Princeton Plasma Physics Laboratory. We also thank Dr. Kurt Polzin for his valuable insight into the FARAD project.

References

[1]C.L.Dailey and R.H. Lovberg. Large diameter inductive plasma thrusters. Number AIAA 79-2093, oct 1979.

[2]K. A. Polzin and E. Y. Choueiri. Performance optimization criteria for pulsed inductive plasma acceleration. *IEEE Transactions on Plasma Science*, 34(3):945–953, 2006.

[3]R. G. Jahn. *Physics of Electric Propulsion.* McGraw-Hill Book Company, 1968.

[4]E. Y. Choueiri and K. A. Polzin. Faraday Acceleration with Radio-frequency Assisted Discharge. *Journal of Propulsion and Power*, 22(3):611–619, May-June 2006.

[5]C.L. Dailey and R.H. Lovberg. Current sheet structure in an inductive-impulsive plasma accelerator. *AIAA Journal*, 10(2):125–192, Feb. 1972.

[6]R.H.Lovberg C.L.Dailey. PIT Mark V design. Number AIAA 91-3571, 1991.

[7]Hallock, A. K. Choueiri, E. Y. and Polzin, K. A. . Current sheet formation in a conical theta pinch faraday accelerator with radio-frequency assisted discharge. Number IEPC-2007-165, September 2007.

[8]R.H. Lovberg and C.L. Dailey. A PIT primer. Technical Report 005, RLD Associates, Encino, CA, 1994.

[9]C.L. Dailey and R.H. Lovberg. The PIT MkV Pulsed Inductive Thruster. Technical Report 191155, Lewis Research Center, Redondo Beach, CA, July 1993.

[10]Hallock, A. K. Choueiri, E. Y. and Polzin, K. A. . Current sheet formation in a conical theta pinch faraday accelerator with radio frequency assisted discharge. Number AIAA-2008-5201, July 2008.